

Theoretical Study of Ln(III) Complexes with Polyaza-Aromatic Ligands: Geometries of $[\text{LnL}(\text{H}_2\text{O})_n]^{3+}$ Complexes and Successes and Failures of TD-DFT

F. Gutierrez,^{*,†,‡} C. Rabbe,[†] R. Poteau,[‡] and J. P. Daudey[‡]

CEA/Valrhô, Atalante, BP 17171, F-30207 Bagnols/Cèze Cedex, France, and Laboratoire de Physique Quantique – UMR 5626, Université Paul Sabatier, 118 route de Narbonne, F-31062 Toulouse Cedex, France

Received: November 15, 2004; In Final Form: March 8, 2005

The accuracy and the usefulness of density functional theory (DFT) and time-dependent density functional theory (TD-DFT) calculations for the theoretical study of Ln (La, Eu, Lu) complexes have been investigated. The geometries calculated at the DFT level for $[\text{Ln}(\text{H}_2\text{O})_n\text{L}]^{3+}$ complexes have been successfully compared with crystallographic data. TD-DFT is able to offer valuable insights into VUV spectra of lanthanide complexes. However, the results obtained on the largest ligand (i.e., 2,4,6-tri-(pyridin-2-yl)-1,3,5-triazine (Tptz)) have to be considered as a failure of TD-DFT.

1. Introduction

In the field of nuclear fuels reprocessing, one possible route is the transmutation of the long-lived minor actinides, such as americium, into short-lived isotopes by irradiation with neutrons.¹ To achieve this goal, it is necessary to separate the trivalent minor actinides (An(III)) from the other elements present in spent fuels (fission products), and especially from the trivalent lanthanides (Ln(III)). This is not a simple task because of the similar chemical properties of these two groups of elements and because Ln(III) amounts to about one-third of the total fission products inventory. An(III)/Ln(III) group separation may be achieved by liquid–liquid extraction systems involving soft-donor extractants.² Recently, polyaza-aromatic compounds have been shown to extract actinides selectively from lanthanides.^{3–6} The investigation of factors affecting the complexes' stability and the understanding of metal–ligand interaction is of great importance in the design of new ligands.

In that context, quantum chemistry calculations in the gas phase could be used in order to understand the interactions between cations and N-bearing ligands better. The present paper reports, as a first step of our progressive methodology, the investigation of the reliability of such methods to determine some properties of $[\text{LnL}(\text{H}_2\text{O})_n]^{3+}$ complexes with L = N-donor ligands and Ln = La, Eu, and Lu. Four ligands were chosen: 2,2':6':2''-terpyridine, named Tpy, 2,4,6-tri-(pyridin-2-yl)-1,3,5-triazine, named Tptz, 2,6-bis-(pyridin-2-yl)-4-amino-1,3,5-triazine, named Adptz, and 2,6-bis-(1,2,4-triazin-3-yl)-pyridine, named Btp (Figure 1). Coordination numbers (CN) of 9 and 8 were considered for La(III) and Lu(III) complexes, respectively. For Eu(III) complexes, CN of both 8 and 9 were considered by varying the number of coordinated water molecules ($n = \text{CN} - 3$) because Eu is in the middle of the lanthanide series where a change in coordination numbers is often observed. As an example, in the series of $[\text{Ln}(\text{Tpy})\text{Cl}(\text{H}_2\text{O})_n]^{2+}$ complexes studied by Kepert et al.,⁷ the coordination number observed for Eu is 8.45.

In the first part, we have optimized the geometry of the complexes at the HF and DFT levels. Relativistic effective core

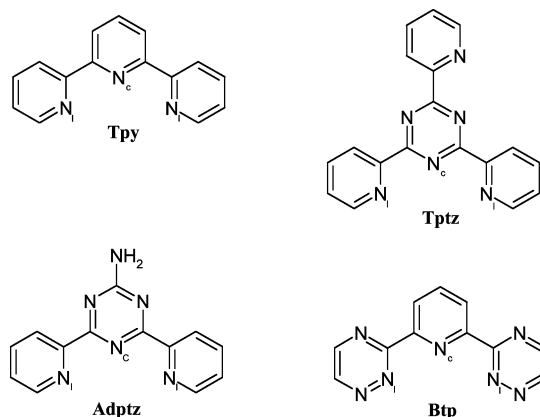


Figure 1. Formulas of the four studied ligands: Tpy, Tptz, Adptz, and Btp.

potential (RECP) methods were chosen to study the electronic structure of Ln complexes. The calculated geometry of the complexes was compared to available X-ray data. In the second part, the excitation spectra of some of these complexes were calculated by using time-dependent density functional theory (TD-DFT)^{8,9} methods and were compared to experimental UV–vis spectra in solution. TD-DFT has been widely used to calculate excited states of molecules with an accuracy comparable to that of CAS-PT2 calculations¹⁰ at least for the lowest part of the spectrum. The main problem with TD-DFT methods is the treatment of charge-transfer (CT) states,^{11,12} Rydberg states, and some excited states of large π molecules^{13,14} due to the incorrect limit of dissociation of the exchange–correlation functional (i.e., the local character of the exchange cannot correctly account for the intrinsic nonlocal nature of CT states). To our knowledge, although TD-DFT has been able to reproduce and interpret the UV–vis spectra^{15–19} of large organic compounds and d-metal complexes, it has never been tested on such Ln complexes.

2. Computational Details

The calculations were carried out at the Hartree–Fock (HF) and density functional theory (DFT) levels of theory with the Gaussian 98 package.²⁰ Full geometry optimization of all

* Corresponding author. E-mail: fabien.gutierrez@laposte.net.

[†] CEA/Valrhô.

[‡] Université Paul Sabatier.

TABLE 1: Comparison of $[\text{Ln}(\text{L})(\text{H}_2\text{O})_n]^{3+}$ Calculated Structures (HF/B3LYP) and X-ray Available Experimental Structures, where N_c and N_l Stand for Central and Lateral Coordinating Nitrogens, Respectively

		La			Eu			Lu				
		calcd		exptl	calcd		exptl	calcd		exptl		
		HF B3LYP			HF B3LYP			HF B3LYP				
		CN = 9		CN = 9	CN = 8		CN = 9	CN = 8		CN = 8		
Tpy	Ln– N_c (Å)	2.69	2.67	2.69 ^a	2.53	2.51	2.59	2.56	2.54 ^b	2.42	2.40	2.44 ^c
	Ln– N_l (Å)	2.69	2.65	2.66 ^a	2.55	2.53	2.60	2.57	2.55 ^b	2.46	2.44	2.46 ^c
	Ln–O (Å)	2.69	2.67	2.56 ^a	2.55	2.53	2.59	2.57	2.48 ^b	2.45	2.42	2.31 ^c
		CN = 9		CN = 10	CN = 8		CN = 9	CN = 10		CN = 8	CN = 10	
Tptz	Ln– N_c (Å)	2.63	2.60	2.66 ^d	2.47	2.45	2.52	2.49	2.54 ^e	2.36	2.34	2.43 ^f
	Ln– N_l (Å)	2.72	2.70	2.70 ^d	2.60	2.57	2.64	2.62	2.59–2.63 ^e	2.51	2.49	2.48–2.50 ^f
	Ln–O (Å)	2.69	2.66	2.49 ^d	2.55	2.52	2.59	2.56	2.40 ^e	2.44	2.42	2.29 ^f
		CN = 9		CN = 10	CN = 8		CN = 9	CN = 9		CN = 8	CN = 9	
Adptz	Ln– N_c (Å)	2.62		2.58 ^g			2.52		2.53 ^h	2.36		2.44 ⁱ
	Ln– N_l (Å)	2.72		2.63–2.64 ^g			2.63		2.58–2.59 ^h	2.51		2.49–2.53 ⁱ
	Ln–O (Å)	2.70		2.48 ^g			2.59		2.38–2.36 ^h	2.45		2.29–2.30 ⁱ
		CN = 9		CN = 8		CN = 9		CN = 8				
Btp	Ln– N_c (Å)	2.77	2.75		2.60	2.60	2.65	2.64		2.49	2.49	
	Ln– N_l (Å)	2.72	2.73		2.57	2.60	2.62	2.62		2.49	2.49	
	Ln–O (Å)	2.66	2.62		2.52	2.48	2.55	2.52		2.41	2.38	

^a $[\text{La}(\text{Tpy})(\text{H}_2\text{O})_5\text{Cl}]^{2+}$, ^b $[\text{Eu}(\text{Tpy})(\text{H}_2\text{O})_5\text{Cl}]^{2+}$, ^c $[\text{Lu}(\text{Tpy})(\text{H}_2\text{O})_4\text{Cl}]^{2+}$, ^d $[\text{Ce}(\text{Tptz})(\text{NO}_3)_3(\text{H}_2\text{O})]^{2+}$, ^e $[\text{Gd}(\text{Tptz})(\text{NO}_3)_3(\text{H}_2\text{O})]^{2+}$, ^f $[\text{Lu}(\text{Tptz})(\text{NO}_3)_3(\text{H}_2\text{O})]^{2+}$, ^g $[\text{La}(\text{Adptz})(\text{NO}_3)_3(\text{H}_2\text{O})]^{2+}$, ^h $[\text{Eu}(\text{Adptz})(\text{NO}_3)_2(\text{H}_2\text{O})_2]^{2+}$, ⁱ $[\text{Lu}(\text{Adptz})(\text{NO}_3)_2(\text{H}_2\text{O})_2]^{2+}$.

molecular systems was carried out without symmetry constraints. Considering that 4f electrons of lanthanide cations do not participate very much in the reactivity of these elements^{21,22} and in order to reduce the computational time, the choice of large core quasi-relativistic effective core potentials (RECP) was made. Calculations were made using ECPs from Stuttgart^{23,24} for Ln atoms, where 46 + 4fⁿ electrons are included in the core. We modeled the lanthanide III ions as 11-valence-electron systems. The contracted (7s6p5d)/[5s4p3d]-GTO²⁴ valence basis set was used for the lanthanides, and the polarized all-electron 6-31G(d) basis set was used for all other atoms. Calculations of the 40 lowest singlets were carried out in the framework of TD-DFT using LDA and B3LYP functionals on the HF-optimized structures of the ground state. We have determined from test cases that using DFT-optimized structures does not significantly modify absorption spectra. The LDA functional is known to give a reliable description of the excited states whose energies lie under $-\epsilon^{\text{HOMO}}$, where $-\epsilon^{\text{HOMO}}$ is the highest occupied molecular orbital energy obtained in the Kohn–Sham description of the ground state.²⁵ In our case, the $-\epsilon^{\text{HOMO}}$ limit is 227 nm for the free ligands and 80 nm for the complexes. The discrete spectra were convoluted with Gaussian functions to reproduce the bandwidth of the experimental spectra (obtained at 298 K in a 76% methanol/24% water medium)²⁶ within the 200–400 nm range.

3. Results and Discussion

3.1. Structure of $[\text{LnL}(\text{H}_2\text{O})_n]^{3+}$ Complexes. The calculated geometries at both the HF and B3LYP levels of theory of $[\text{LnL}(\text{H}_2\text{O})_n]^{3+}$ complexes were compared to available experimental structures.^{4,7,27} Table 1 shows some geometrical features (Ln–N and Ln–O_{water} bond lengths) for Tpy, Tptz, Adptz, and Btp complexes. Note that the experimental structures of Ln(III) complexes displayed in Table 1 are somehow different from the calculated complexes because of the lack of experimental structures strictly identical to those considered in those series of complexes. Those differences arise from the molecules present in the first coordination sphere or from a different

coordination number. This is due to the complexity of obtaining such 1:1 complexes in nitric acid as the solvent. The interest in making calculations on this set of ligands across a Ln series (Ln = La, Eu, Lu) is directed toward obtaining general trends, as will be shown. The ligand Adptz was studied partially to allow comparison with other similar ligands because experimentally it shows a weak stability to radiolysis. As shown in Table 1, experimental distances between the metal ion and the ligand L are correctly reproduced by these calculations with an accuracy of a few hundredths of an angstrom. It should be mentioned that other parameters as angles and dihedrals, not given here, are also in agreement with the experimental data. Moreover, the lanthanide contraction is well taken into account by the calculations, as shown by the decrease in Ln–ligand bond lengths when going from La(III) to Lu(III). HF and DFT results are very similar for the bond length, whereas DFT performs better for angles and dihedrals. This fair agreement between those methods may be due to softer correlation effects observed in ionic bonds rather than in covalent ones. In most cases, Ln–N distances are closer to experimental values than Ln–O distances: water molecules are very mobile and therefore very sensitive to the chemical environment in the first coordination sphere.²⁸ Indeed, the difference between the calculated and experimental Ln–O distances is larger for Tptz and Adptz (for which the experimental structures involve nitrate ions in the first coordination sphere) than for Tpy complexes. However, it has to be noticed that such calculations tend to overestimate these distances slightly: calculations for La(III), Eu(III), and Lu(III) hydrated ions²⁹ (not shown here) give Ln–O distances that are longer by about 0.08 Å (HF) and 0.05 Å (B3LYP) compared to experimental data.²⁷

The lack of experimental data for La, Eu, or Lu complexes of Btp ligands did not allow us to compare them directly to the calculated structures of $[\text{Ln}(\text{Btp})(\text{H}_2\text{O})_n]^{3+}$. However, two experimental structures are available for the Nd(III) ion, $[\text{Nd}(\text{Et}_4\text{Btp})(\text{NO}_3)_3(\text{EtOH})]$ and $[\text{Nd}(\text{nPr}_4\text{Btp})(\text{NO}_3)_4]^{-}$.^{30–32} The calculated Ln–N distances for La(III) and Eu(III) complexes are (as expected because the two ions are close to Nd(III) in

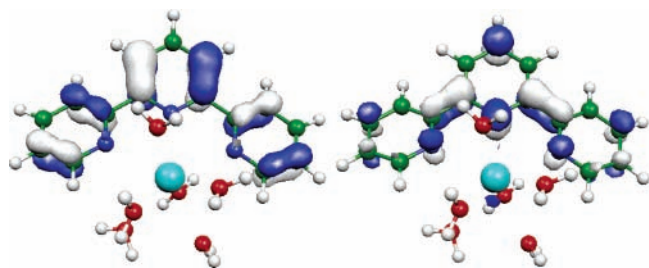


Figure 2. HOMO–LUMO intense transition in the Tpy La complex.

the lanthanide series) longer and shorter, respectively, than those experimentally observed with Nd(III) complexes, in accordance with the lanthanide contraction.

The distances from B3LYP calculations are generally in better agreement with experimental data than those from HF calculations. The same trend between B3LYP and HF can be observed for dihedral angles. If one looks carefully at the Ln–N distances between ligands and lanthanide cations, B3LYP calculations provide a reasonable estimation of CN. As a matter of fact, in the case of the Tpy ligand, we have performed calculations with the same CN as for the molecules analyzed by means of X-rays. It appears that the Ln–N_c and Ln–N_l distances are a good probe for CN: the largest difference is found for Lu (0.04 Å). Concerning the Tptz ligand coordinated to Eu, one can see in Table 1 that whereas the Eu–N_l distance is insensitive to the number of water molecules in the first coordination sphere the Eu–N_c distance tends toward the experimental value when CN varies from 8 to the experimental CN (i.e., CN = 10); the difference between X-ray data and theoretical results is 0.14 Å for CN = 8 and 0.04 Å for CN = 9. Concerning Lu–Tptz complexes, we have considered only CN = 8, whereas the experimental evidence is CN = 10.

Again, although the Lu–N_l distance is already close to the X-ray data, the Ln–N_c one is far from experiments (2.34 vs 2.43 Å). However, it appears that the theoretical models we used are not yet able to provide geometries that are accurate enough to determine the coordination number of middle lanthanide series complexes because the interactions with other coordination spheres is very important in predicting such a property correctly. Therefore, it would be interesting to enclose these systems in a box of water molecules by means of QM/MM methods and to consider the dynamical effects.

3.2. Theoretical Spectroscopy of [LnL(H₂O)_n]³⁺ Complexes. Calculations have been carried on lanthanide complexes of coordination number of 9 for lanthanum, 8 for lutecium, and for both coordination number for europium, which is in the middle of the lanthanide series at the HF and/or DFT level.

LDA. The most intense bands are without exception the $\pi\pi^*$ type and are for ligand–ligand transitions, as shown in Figure 2. Some excitations of minor intensity involve virtual d orbitals of the lanthanide, as in the case of Tpy (Figure 3). The change in the intensity of the free ligand and the complex shows the participation of the central N atom in the bonding of the Ln³⁺ cation. As can be seen in Figure 4, the respective intensity of the various bands and the position of the bands are not correct, clearly showing the limitation of the LDA functional. Better quantitative results would be expected with more efficient functionals such as B3LYP.

Btp Complexes. From a theoretical point of view, the hydrated complexes show the same number of bands (Figure 4). Along the Ln series, the λ_{max} of all of the bands increases by a few nanometers. In comparison with experimental data, a similar structure of bands can be observed, despite the fact that some

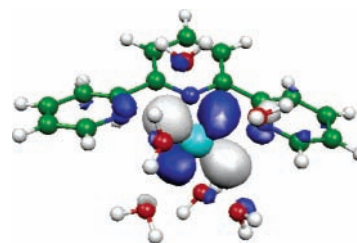


Figure 3. Virtual d orbital of the Tpy La complex involved in low- and high-intensity transitions in LDA and B3LYP calculations, respectively.

discrepancies are noticed between the relative intensities of the bands. The bands are blue shifted with respect to experimental ones by approximately 30 nm. The excitation located around 250 nm always involves the coordinating central N atom of the ligand. The most intense transitions are of charge-transfer character from the π orbital located on the central ring to π^* orbitals based on lateral rings of the ligand. The increase in intensity when going from the free ligand to the Ln complexes is related to a more important contribution of the coordinating central N atom, showing the major role of this atom in the bonding with the Ln³⁺ cation. In the case of the five-hydrated Lu(III) complex, the theoretical spectra exhibits the same structure as the six-hydrated one, but with the broken symmetry of the π^* orbitals located only on one lateral ring.

Tpy Complexes. As in the Btp case, the free ligand and the complexes show the same number of bands and the same shift along the Ln(III) series with a noticeable change in the relative intensities (Figure 4). The transition located around 350 nm is always based on the HOMO and LUMO orbitals with $\pi\pi^*$ character (Figure 2). Some transitions observed at 230 nm or at shorter wavelengths correspond to excitations from the π orbital to virtual d orbitals (Figure 3) of the lanthanides in the case of Eu(III) and Lu(III). These LMCT states significantly contribute to the overall intensity of the high-energy band. The theoretical spectra appear shifted in all the cases by approximately 30 nm.

Tptz Complexes. The theoretical spectra of the Tptz ligand and complexes convoluted with 40 singlets ranges from 200 to 600 nm. No experimental spectra were detected from 400 to 600 nm, thus leading to a large disagreement with our theoretical calculations, which predict for the complexes the presence of medium bands in this range. Those bands observed at longer wavelengths in the complex are not observed in the free ligand. The excited states in the range of 400–600 nm are described by CT transitions between the lateral rings of the ligand. As a matter of fact, the supplementary ring compared with the other ligands leads to a wider variety of $\pi\pi^*$ states with excitations based on the upper ring to the lateral rings or from the central one to the lateral ones. Excitations to virtual d orbitals of Ln are also observed all along the series.

Considering that TD-LDA leads to the wrong spectrum, the theoretical interpretation of the UV bands in the framework of that method is questionable.

B3LYP. From our experience³³ with the analysis of TD-B3LYP spectra from benzophenone and its derivatives, there is a smaller difference between the theoretical transition wavelength and the experimental ones than in the TD-LDA case; thus, the assignment of the bands is certainly more reliable.

Tpy Complexes. The free ligand experimentally exhibits an intense and broad band at 232 nm, which is predicted to be at 246 nm (Figure 5). A new band appears in the Ln complexes around 320 nm corresponding to a HOMO–LUMO transition

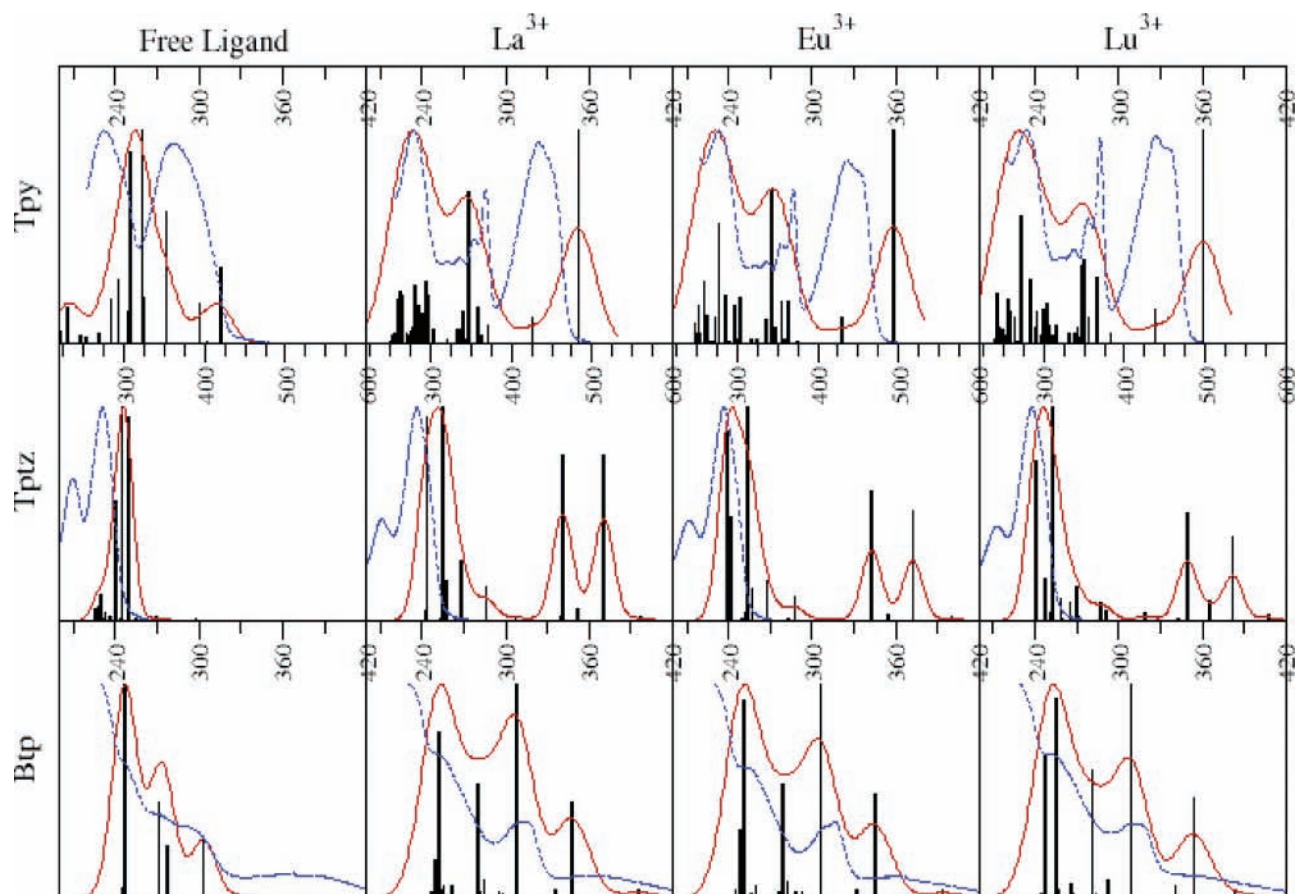


Figure 4. Comparison of experimental spectra (dashed lines) for free ligands and complexes with theoretical LDA spectra (solid lines).

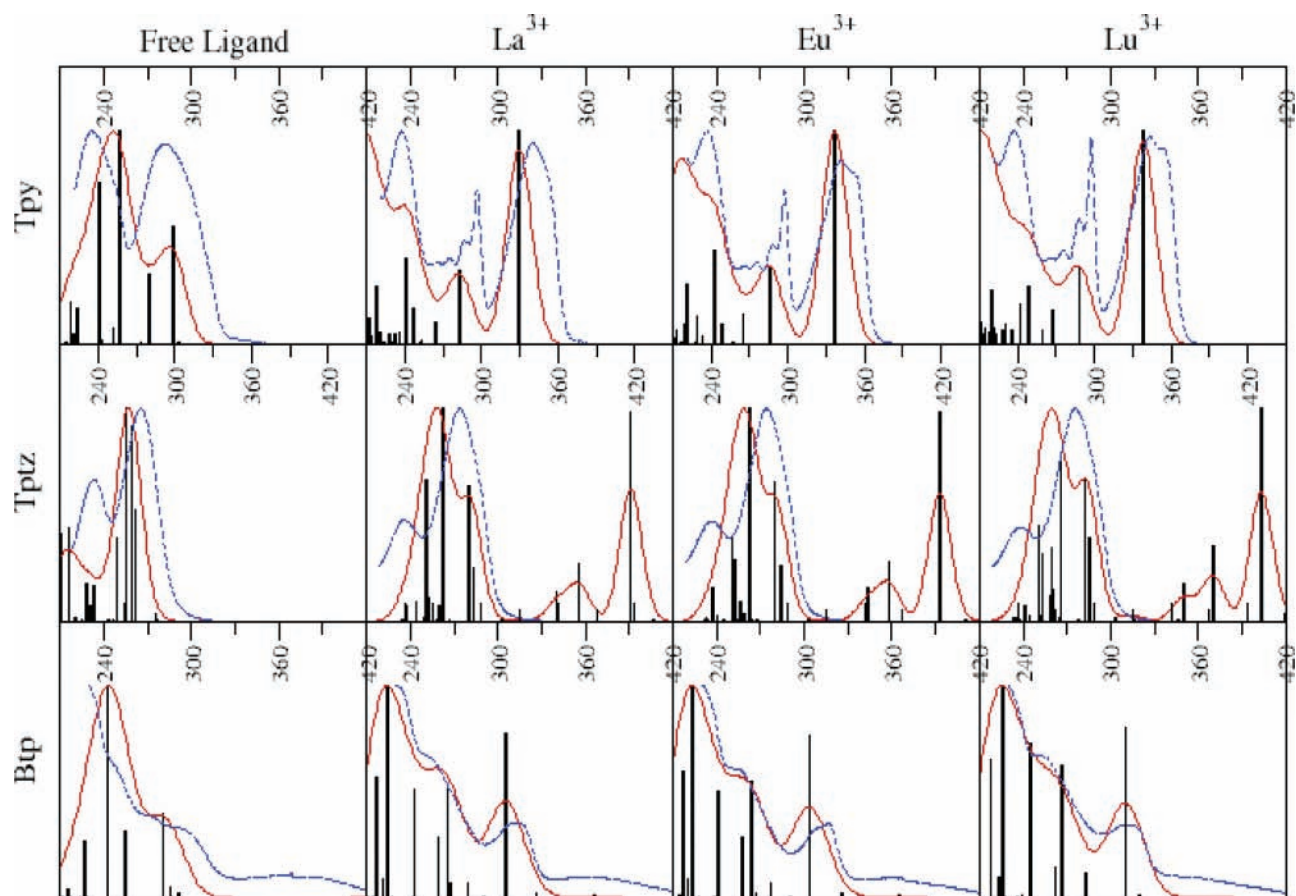


Figure 5. Comparison of experimental spectra (dashed lines) for free ligands and complexes with theoretical B3LYP spectra (solid lines).

of $\pi\pi^*$ character. The theoretical spectrum around 275 nm is unable to represent the sharp structure of the experimental one, which nevertheless may be a vibrational substructure. Intense transitions at wavelengths lower than 200 nm are predicted to be from π to virtual d orbitals of the lanthanide type. This is a major difference with the TD-LDA results, where those transitions were always very weak. There is still a small blue shift between the theoretical wavelength and the experimental ones, but it is now rather small (i.e., <15 nm). The relative intensities of the bands are improved with respect to TD-LDA results.

Btp Complexes. The assignment is made as easily as for the previous ligand. The experimental spectra and the theoretical ones are superimposed, showing the same relative intensities and a very small shift. The experimental spectra after 325 nm do not show a rapid decrease to the baseline. From our calculation, an excitation at 366 nm of $n\pi^*$ character is involved and explains the weak intensity of this type of transition. The strengthening of some transitions between the free ligand and the complexes can be clearly assigned to a more important contribution of the nitrogen atoms.

Tptz Complexes. The Tptz ligand is the largest π system of this study. The experimental spectrum of the free ligand shows the same number of bands as the theoretical one (Figure 5). The relative intensities of the theoretical band and the experimental band located around 275 nm are inverted. Experimentally, no absorption spectra were observed in the 325–500 nm range, whereas TD-B3LYP calculations predict excitations with large intensities in this domain, as in the LDA case. The presence of bands in the complex that do not correspond to the free ligand cannot be attributed to any major difference in the geometry of both species because they remain planar with few changes in the angles around the coordinating site. Looking further into the nature of those transitions clearly shows that both are π orbitals on the upper ring of the Tptz ligand to the LUMO orbital. This LUMO orbital is of π^* character, mainly based on the central ring with small contributions of the lateral and the upper cycles. Those spurious states are likely to come from the fact that TD-DFT is an approximate method due to the nonexact nature of the exchange-correlation functional.^{12,14} This hypothesis is partially corroborated by additional calculations carried out at the same level on the TptzLaCl₃ system. As a matter of fact, the substitution of water molecules by chlorine atoms drastically modifies the long-range electrostatic interactions. The low-energy states, which can be considered to be spurious, are very sensitive to this substitution, although they are strictly localized on the Tptz ligand. They are still present in the TptzLaCl₃ complex, but with very weak intensities leading to no absorption band, and are based on chlorine excitations. Evidence of the failure of TD-DFT for CT excited states of large π molecules has been in particular shown by Dreuw et al.³⁴ in the case of bacteriochlorin and bacteriochlorophyll complexes. These authors have shown that the lowest CT states are dramatically underestimated by approximately 2 eV. The exchange-correlation potential decays faster than $1/R$, leading to the inability to describe this kind of excitation safely. Further investigations have been carried out using functionals with a correct dissociation limit such as LB94³⁵ and the so-called Casida–Salahub³⁶ correction (CS00) with the NWChem^{37,38} package. No improvements of the intensity and of the position of the spurious states were observed using those functionals. If we eliminate the spurious states of Tptz complexes, then TD-B3LYP calculations are always in better agreement with experiments for the energy of the transition than in the TD-

LDA case. The relative intensities of the bands are in most cases well described.

4. Conclusions

DFT calculations have been able to fairly reproduce structures of Ln(III) complexes more accurately than HF and have revealed the main importance of the first coordination sphere. The distance between water molecules and Ln(III) was always overestimated whatever the method used.

TD-LDA calculations on free ligands and complexes have shown various discrepancies between theory and experiment coming from the intensity ratio between excitations, which may give rise to supplementary bands. TD-LDA spectra always show a larger shift than TD-B3LYP according to experimental data.

In contrast, TD-B3LYP spectra are systematically closer to experimental ones considering the wavelength and relative intensities of bands. Consequently, insofar as agreement between theory and experiment is achieved, TD-B3LYP calculations can provide theoretical insights into the nature of the excitations involved in the observed bands.

However, several charge-transfer-type excitations have been characterized with a strong intensity leading to unobserved bands. Those excitations are poorly described by the usual functionals and may give energy shifts of several eV, therefore producing such unobserved bands.

This casts suspicion on TD-DFT calculations used with popular functionals. TD-B3LYP appears to be an interesting tool for rationalizing VUV spectra but cannot be used for predicting spectra in the framework of molecular design without a careful analysis of the results.

Acknowledgment. F.G. and R.P. thank the CALcul en Midi-Pyrénées (CALMIP) and the Centre Informatique National de l'Enseignement Supérieur (CINES) for the allocation of computational resources.

References and Notes

- (1) Proceedings of the Fifth OECD/NEA International Information Exchange Meeting on Actinide and Lanthanide Product Partitioning and Transmutation, Mol, Belgium, Nov 25–27, 1998.
- (2) Nash, K. L. *Solvent Extr. Ion Exch.* **1993**, *11*, 729.
- (3) Cordier, P. Y.; Hill, C.; Baron, P.; Madic, C.; Hudson, M. J.; Liljenzin, J. O. *J. Alloys Compds.* **1998**, *271*, 738.
- (4) Drew, M. G. B.; Hudson, M. J.; Iveson, P. B.; Madic, C.; Russel, M. L. *J. Chem. Soc., Dalton Trans.* **2000**, 2711.
- (5) Drew, M. G. B.; Iveson, P. B.; Hudson, M. J.; Liljenzin, J. O.; Spjuth, L.; Cordier, P. Y.; Enarsson, A.; Hill, C.; Madic, C. *J. Chem. Soc., Dalton Trans.* **2000**, 821.
- (6) Zolarik, Z.; Müllich, U.; Gassner, F. *Solvent Extr. Ion Exch.* **1999**, *17*, 23.
- (7) Kepert, C. J.; Weimin, L.; Skelton, B. W.; White, A. H. *Aust. J. Chem.* **1994**, *47*, 365.
- (8) Burke, K.; Gross, E. K. U. A Guided Tour of Time-Dependent Density Functional Theory. In *Density Functionals: Theory and Applications*; Springer: Berlin, 1998; p 117.
- (9) Jamorski, C.; Casida, M. E.; Salahub, D. R. *J. Chem. Phys.* **1996**, *104*, 5134.
- (10) Tozer, D. J.; Amos, R. D.; Handy, N. C.; Roos, B. O.; Serrano-Andres, L. *Mol. Phys.* **1999**, *97*, 859.
- (11) Casida, M. E.; Gutierrez, F.; Guan, J.; Gadea, F. X.; Salahub, D.; Daudey, J. P. *J. Chem. Phys.* **2000**, *113*, 7062.
- (12) Dreuw, A.; Weisman, J. L.; Head-Gordon, M. *J. Chem. Phys.* **2003**, *119*, 2943.
- (13) Cai, Z.-L.; Sendt, K.; Reimers, J. R. *J. Chem. Phys.* **2002**, *117*, 5543.
- (14) Grimme, S.; Parac, M. *ChemPhysChem* **2003**, *3*, 292.
- (15) Bauernschmitt, R.; Ahlrichs, R.; Hennrich, F. H.; Kappes, M. M. *J. Am. Chem. Soc.* **1998**, *120*, 5052.
- (16) Ginsberg, S. J. A.; Rosa, A.; Ricciardi, G.; Baerends, E. J. *J. Chem. Phys.* **1999**, *111*, 2499.
- (17) Adamo, C.; Barone, V. *Theor. Chim. Acta* **2000**, *105*, 169.

- (18) Lhiaubet, V.; Gutierrez, F.; Pennaud-Berruyer, F.; Amouyal, E.; Daudey, J. P.; Poteau, R.; Chouini-Lalanne, N.; Paillous, N. *New J. Chem.* **2000**, *24*, 403.
- (19) Ciofini, I.; Daul, C. A.; Adamo, C. *J. Phys. Chem. A* **2003**, *107*, 11182.
- (20) Frisch, M. J.; Trucks, G. W.; Schlegel, H. B.; Scuseria, G. E.; Robb, M. A.; Cheeseman, J. R.; Zakrzewski, V. G.; Montgomery, J. A., Jr.; R. E. S.; Burant, J. C.; Dapprich, S.; Millam, J. M.; Daniels, A. D.; Kudin, K. N.; Strain, M. C.; Farkas, O.; Tomasi, J.; Barone, V.; Cossi, M.; Cammi, R.; Mennucci, B.; Pomelli, C.; Adamo, C.; Clifford, S.; Ochterski, J.; Petersson, G. A.; Ayala, P. Y.; Cui, Q.; Morokuma, K.; Malick, D. K.; Rabuck, A. D.; Raghavachari, K.; Foresman, J. B.; Cioslowski, J.; Ortiz, J. V.; Baboul, A. G.; Stefanov, B. B.; Liu, G.; Liashenko, A.; Piskorz, P.; Komaromi, I.; Gomperts, R.; Martin, R. L.; Fox, D. J.; Keith, T.; Al-Laham, M. A.; Peng, C. Y.; Nanayakkara, A.; Gonzalez, C.; Challacombe, M.; Gill, P. M. W.; Johnson, B. G.; Chen, W.; Wong, M. W.; Andres, J. L.; Head-Gordon, M.; Replogle, E. S.; Pople, J. A. *Gaussian 98*, revision A.9; Gaussian, Inc.: Pittsburgh, PA, 1998.
- (21) Maron, L.; Eisenstein, O. *J. Phys. Chem. A* **2000**, *104*, 7140.
- (22) Adamo, C.; Maldivi, P. *Chem. Phys. Lett.* **1997**, *268*, 61.
- (23) Dolg, M.; Stoll, H.; Preuss, H. *Theor. Chim. Acta* **1993**, *85*, 441.
- (24) Dolg, M.; Stoll, H.; Savin, A.; Preuss, H. *Theor. Chim. Acta* **1989**, *75*, 173.
- (25) Casida, M. E.; Jamorski, C.; Casida, K. C.; Salahub, D. R. *J. Chem. Phys.* **1998**, *108*, 4439.
- (26) François, N. Towards an Interpretation of the Mechanism of the An(III)/Ln(III) Separation by Synergistic Solvent Extraction with Nitrogen-Containing Polydentate Ligands. Université Henri Poincaré, 1999.
- (27) Grigoriev, M.; Den Auwer, C.; Berthon, L.
- (28) Derepas, A. L.; Soudan, J. M.; Brenner, V.; Dognon, J. P.; Millié, P. *J. Comput. Chem.* **2002**, *23*, 1014.
- (29) Rabbe, C.; Gutierrez, F. Etude par chimie quantique de complexes $[\text{LnL}(\text{H}_2\text{O})_n]^{3+}$.
- (30) Habenschuss, A.; Spedding, F. H. *J. Chem. Phys.* **1979**, *70*, 2797.
- (31) Habenschuss, A.; Spedding, F. H. *J. Chem. Phys.* **1979**, *70*, 3758.
- (32) Habenschuss, A.; Spedding, F. H. *J. Chem. Phys.* **1979**, *73*, 442.
- (33) Gutierrez, F. Etude Théorique des États Excités de Grandes Molécules. Université Paul Sabatier, 2002.
- (34) Dreuw, A.; Head-Gordon, M. *J. Am. Chem. Soc.* **2004**, 4007.
- (35) van Leeuwen, R.; Baerends, E. *J. Phys. Rev. A* **1994**, *49*, 2421.
- (36) Casida, M. E.; Jamorski, C.; Casida, K. C.; Salahub, D. R. *J. Chem. Phys.* **1998**, *108*, 4439.
- (37) Kendall, R. A.; Aprà, E.; Bernholdt, D. E.; Bylaska, E. J.; Dupuis, M.; Fann, G. I.; Harrison, R. J.; Ju, J.; Nichols, J. A.; Nieplocha, J.; Straatsma, T. P.; Windus, T. L.; Wong, A. T. *Comput. Phys. Commun.* **2000**, *128*, 260.
- (38) Straatsma, T. P.; Aprà, E.; Windus, T. L.; Bylaska, E. J.; de Jong, W.; Hirata, S.; Valiev, M.; Hackler, M. T.; Pollack, L.; Harrison, R. J.; Dupuis, M.; Smith, D. M. A.; Nieplocha, J.; V., T.; Krishnan, M.; Auer, A. A.; Brown, E.; Cisneros, G.; Fann, G. I.; Fruchtl, H.; Garza, J.; Hirao, K.; Kendall, R.; Nichols, J.; Tsemekhman, K.; Wolinski, K.; Anchell, J.; Bernholdt, D.; Borowski, P.; Clark, T.; Clerc, D.; Dachselt, H.; Deegan, M.; Dyall, K.; Elwood, D.; Glendening, E.; Gutowski, M.; Hess, A.; Jaffe, J.; Johnson, B.; Ju, J.; Kobayashi, R.; Kutteh, R.; Lin, Z.; Littlefield, R.; Long, X.; Meng, B.; Nakajima, T.; Niu, S.; Rosing, M.; Sandrone, G.; Stave, M.; Taylor, H.; Thomas, G.; van Lenthe, J.; Wong, A.; Zhang, Z. *NWChem, A Computational Chemistry Package for Parallel Computers*, version 4.6; Pacific Northwest National Laboratory: Richland, WA, 2004.